Hybrid Beamforming with One-Bit Quantized Phase Shifters in mmWave MIMO Systems

Zihuan Wang†, Ming Li†, Hongyu Li†, and Qian Liu‡
†School of Information and Communication Engineering
Dalian University of Technology, Dalian, Liaoning 116024, China
E-mail: {wangzihuan,hongyuli}@mail.dlut.edu.cn, mli@dlut.edu.cn
‡ School of Computer Science and Technology
Dalian University of Technology, Dalian, Liaoning 116024, China
E-mail: qianliu@dlut.edu.cn

***Abstract*—Economical and energy-efficient analog/digital hybrid beamforming has been widely considered as a promising approach for millimeter wave (mmWave) multiple-input multiple-output (MIMO) systems. While most hybrid beamforming techniques consider a fully-connected structure with a large number of phase shifters (PSs), the partially-connected structure has drawn more attention recently since it requires much less PSs and can further improve energy-efficiency. However, the impractical assumption of infinite or high resolution of PSs in existing solutions frustrates the real-world deployment of hybrid beamforming designs, and low-resolution PSs are typically adopted to reduce the hardware complexity and power consumption. In an effort to achieve maximum hardware efficiency, this paper focuses on the partially-connected architecture with *one-bit* (binary) PSs and considers the problem of joint hybrid precoder and combiner design for such mmWave MIMO systems. We propose to successively design the analog beamformers associated with each pair of sub-array, aiming at conditionally maximizing the spectral efficiency. A novel binary analog precoder and combiner optimization algorithm is proposed under a rank-1 approximation of the interference-included equivalent channel with polynomial complexity in the number of antennas. Then, the digital precoder and combiner are computed based on the obtained effective baseband channel to further enhance the spectral efficiency. Simulation results demonstrate the advantages of proposed hardware-efficiency hybrid precoder and combiner design.**

I. Introduction

Millimeter wave (mmWave) communications, operating in frequency bands of 30-300 GHz, have initiated a new era of wireless communications by reducing the spectrum congestion through exploitation of the significantly large mmWave frequency bands [1], [2]. The smaller wavelength of mmWave signals allows for a large antenna array of massive multiple-input multiple-output (MIMO) systems to be integrated in a small device [3]. The large antenna array can provide sufficient beamforming gain with precoding and combining techniques to overcome severe free-space pathloss of mmWave channels.

For conventional MIMO systems operating in microwave frequency bands, full-digital precoder and combiner are realized using a large number of expensive and energy-intensive radio frequency (RF) chains, analog-to-digital converters (ADCs), and digital-to-analog converters (DACs). Due to the ten-fold increase of the carrier frequency and bandwidth in mmWave communications, it is no longer feasible to adopt these full-digital technologies. Recently, economical and energy-efficient analog/digital hybrid beamforming schemes have emerged as a promising approach for mmWave MIMO systems. The hybrid architecture applies a phase shifter (PS) network to implement high-dimensional analog precoder, and a small number of RF chains for low-dimensional digital precoder to provide the necessary flexibility for multiplexing/multiuser techniques.

Fully-connected structure is typically employed to realize hybrid precoders and combiners, which requires a large number of PSs and is still energy-intensive. Therefore, partially-connected architecture has been proposed to reduce the number of PSs and further improve the energy-efficiency [4]. Based on these two architectures, existing hybrid beamforming designs usually assume the infinite-resolution PSs based analog precoders [4]-[6], or the high-resolution codebook based beamformers [7]-[10]. However, it is of high hardware complexity and power consumption to realize accurate or high-resolution PSs. Therefore, more cost effective and energy efficient low-resolution PSs are typically used to implement analog beamformers in practical mmWave MIMO systems. This initiates an important research trend of exploring hybrid beamforming schemes with the low-resolution PSs.

In this paper, we consider the problem of hybrid precoder and combiner design for partially-connected architecture with one-bit (binary) PSs to achieve maximum hardware efficiency. We propose to successively design the analog beamformers for each pair of sub-array, aiming at conditionally maximizing the spectral efficiency. Inspired by the findings in [11], we introduce a novel binary analog precoder and combiner design algorithm under the rank-1 approximation of the interference-included equivalent channel with polynomial complexity in the number of antennas. Then, the digital precoder and combiner are computed based on the obtained effective baseband channel to further enhance the spectral efficiency. Simulation results demonstrate that the proposed algorithm can achieve satisfactory spectral efficiency and higher energy efficiency

This paper is supported by the National Natural Science Foundation of China (Grant No. 61671101 and 61601080) and the Fundamental Research Funds for the Central Universities (Grant No. DUT15RC(3)121 and DUT17JC10).

978-1-5386-3180-5/18/$31.00 ©2018 IEEE

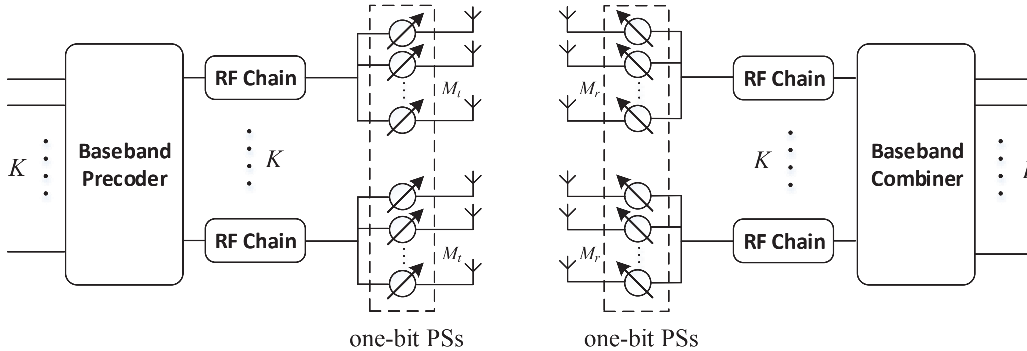

Fig. 1. The mmWave MIMO system using hybrid precoder and combiner based on partially-connected architecture with one-bit quantized PSs.

compared with existing hybrid beamforming schemes using high-resolution PSs.

II. System Model

We consider a partially-connected hybrid beamforming architecture with binary PSs in mmWave MIMO systems, as illustrated in Fig. 1. The transmitter is equipped with K RF chains and N_t antennas. Each data stream is transmitted via a corresponding RF chain and $M_t = \frac{N_t}{K}$ antennas. The receiver employs K RF chains, each of which is connected to M_r antennas to receive the signals, and the total number of receive antennas is $N_r = M_r \times K$.

The discrete-time transmitted signal can be written as

$$\mathbf{x} = \sqrt{P}\mathbf{F}_{RF}\mathbf{F}_{BB}\mathbf{s}, \quad (1)$$

where $\mathbf{s}$ is the $K \times 1$ symbol vector such that $\mathbb{E}\{\mathbf{s}\mathbf{s}^H\} = \frac{1}{K}\mathbf{I}_K$. $\mathbf{F}_{BB} \in \mathbb{C}^{K\times K}$ is the digital precoder and $\mathbf{F}_{RF} \in \mathbb{C}^{N_t \times K}$ is the analog precoder which has the form of

$$\mathbf{F}_{RF} = \begin{bmatrix} \mathbf{f}_{RF,1} & \mathbf{0} & \dots & \mathbf{0} \\ \mathbf{0} & \mathbf{f}_{RF,2} & & \mathbf{0} \\ \vdots & & \ddots & \vdots \\ \mathbf{0} & \mathbf{0} & \dots & \mathbf{f}_{RF,K} \end{bmatrix}, \quad (2)$$

where the non-zero elements are assumed to have a constant amplitude $\frac{1}{\sqrt{M_t}}$ and one-bit (binary) quantized phases for each element, i.e. $\mathbf{f}_{RF,l} \in \frac{1}{\sqrt{M_t}}\{\pm 1\}^{M_t},\ l = 1, \dots, K$. P represents transmit power and the total transmit power constraint is enforced by normalizing $\mathbf{F}_{BB}$ such that $\|\mathbf{F}_{RF}\mathbf{F}_{BB}\|_F^2 = K$.

For simplicity, we consider a narrowband block-fading propagation channel, which yields the received signal as

$$\mathbf{y} = \sqrt{P}\mathbf{H}\mathbf{F}_{RF}\mathbf{F}_{BB}\mathbf{s} + \mathbf{n}, \quad (3)$$

where $\mathbf{y}$ is the $N_r \times 1$ received vector, $\mathbf{H}$ is the $N_r \times N_t$ channel matrix, and $\mathbf{n} \sim \mathcal{CN}(\mathbf{0}, \sigma^2\mathbf{I}_{N_r})$ is the complex Gaussian noise vector corrupting the received signal.

The obtained signal after combining at the receiver has a form of

$$\widehat{\mathbf{s}} = \sqrt{P}\mathbf{W}_{BB}^H\mathbf{W}_{RF}^H\mathbf{H}\mathbf{F}_{RF}\mathbf{F}_{BB}\mathbf{s} + \mathbf{W}_{BB}^H\mathbf{W}_{RF}^H\mathbf{n}, \quad (4)$$

where $\mathbf{W}_{RF} \in \mathbb{C}^{N_r \times K}$ is the analog combiner with similar constraints as $\mathbf{F}_{RF}$, $\mathbf{W}_{BB}$ is the $K \times K$ baseband digital combiner.

The mmWave propagation in a massive MIMO system is well characterized by a limited spatial selectivity or scattering model, e.g. the Saleh-Valenzuela model, which allows us to accurately capture the mathematical structure in mmWave channels [7]. The channel matrix $\mathbf{H}$ is assumed to be a sum contribution of N_{cl} scattering clusters, each of which provides N_{ray} propagation paths to the channel matrix $\mathbf{H}$. Therefore, the discrete-time narrow-band mmWave channel $\mathbf{H}$ can be formulated as

$$\mathbf{H} = \sqrt{\frac{N_t N_r}{N_{c1} N_{ray}}} \sum_{i=1}^{N_{cl}} \sum_{m=1}^{N_{ray}} \alpha_{im}\mathbf{a}_r(\theta_{im}^r)\mathbf{a}_t(\theta_{im}^t)^H, \quad (5)$$

where $\alpha_{im} \sim \mathcal{CN}(0, \sigma_{\alpha,i}^2)$ is the complex gain of the m-th propagation path (ray) in the i-th scattering cluster, following independent identically distributed (i.i.d.) form. Let $\sigma_{\alpha,i}^2$ represent the average power of the i-th cluster, and the total power satisfies $\sum_{i=1}^{N_{cl}} \sigma_{\alpha,i}^2 = N_{c1}$. θ_{il}^t and θ_{il}^r are the angle of departure (AoD) and the angle of arrival (AoA), respectively, which are assumed to be Laplacian-distributed with a mean cluster angle θ_i^t and θ_i^r as well as an angle spread of $\sigma_{\theta_i^t}$ and $\sigma_{\theta_i^r}$. Finally, the array response vectors $\mathbf{a}_r(\theta^r)$ and $\mathbf{a}_t(\theta^t)$ are the antenna array response vectors, which only depend on the antenna array structures. When the commonly used uniform linear arrays (ULAs) are considered, the receive antenna array response vector can be written as

$$\mathbf{a}_r(\theta^r) = \frac{1}{\sqrt{N_r}}[1, e^{j\frac{2\pi}{\lambda}d\sin(\theta^r)}, \dots, e^{j(N_r-1)\frac{2\pi}{\lambda}d\sin(\theta^r)}]^T, \quad (6)$$

where λ is the signal wavelength, and d is the distance between antenna elements. The transmit array response vector $\mathbf{a}_t(\theta^t)$ can be written in a similar fashion. In this paper, we assume perfect timing and frequency recovery and the channel state information (CSI) of $\mathbf{H}$ is perfectly known to both transmitter and receiver. In practice, CSI can be accurately and efficiently obtained by channel estimation at the receiver and further shared at the transmitter with effective feedback techniques.

Based on the partially-connected structure with binary PSs, we aim to jointly design the hybrid precoder and combiner for a mmWave MIMO system to maximize the spectral efficiency. When Gaussian symbols are transmitted over the mmWave

MIMO channel, the achievable spectral efficiency is given by

$$R = \log_2\left(\left|\mathbf{I}_K + \frac{P}{K}\mathbf{R}_n^{-1}\mathbf{W}_{BB}^H\mathbf{W}_{RF}^H\mathbf{H}\mathbf{F}_{RF}\mathbf{F}_{BB} \times \mathbf{F}_{BB}^H\mathbf{F}_{RF}^H\mathbf{H}^H\mathbf{W}_{RF}\mathbf{W}_{BB}\right|\right), \quad (7)$$

where $\mathbf{R}_n \triangleq \sigma_n^2\mathbf{W}_{BB}^H\mathbf{W}_{RF}^H\mathbf{W}_{RF}\mathbf{W}_{BB}$ is the noise covariance matrix after combining.

III. Proposed Hybrid Precoder and Combiner Design

Obviously, the solution to design the hybrid precoder and combiner is not straightforward. In this section, we first focus on the analog precoder and combiner design. Then, having the effective baseband channel associated with the obtained analog precoder and combiner, the digital precoder and combiner are computed to further maximize the spectral efficiency.

A. Analog Precoder and Combiner Design

Under high signal-to-noise-ratio (SNR) circumstance, the achievable spectral efficiency in (7) can be rewritten as

$$R \approx \log_2\left(\left|\frac{P}{K}\mathbf{R}_n^{-1}\mathbf{W}_{BB}^H\mathbf{W}_{RF}^H\mathbf{H}\mathbf{F}_{RF}\mathbf{F}_{BB} \times \mathbf{F}_{BB}^H\mathbf{F}_{RF}^H\mathbf{H}^H\mathbf{W}_{RF}\mathbf{W}_{BB}\right|\right). \quad (8)$$

While the per-antenna SNR in mmWave systems is typically low, the post-combining SNR should be high enough to justify this approximation. In addition, it has been verified in [6] that for large-scale MIMO systems, the optimal analog beamformers are approximately orthogonal, i.e. $\mathbf{F}_{RF}^H\mathbf{F}_{RF} \propto \mathbf{I}_K$. Besides, the near-optimal hybrid design should exhibit orthogonality property as the full-digital solution, i.e. $\mathbf{F}_{BB}^H\mathbf{F}_{RF}^H\mathbf{F}_{RF}\mathbf{F}_{BB} \approx \mathbf{I}_K$. This fact allows us to assume that the digital precoder $\mathbf{F}_{BB}$ is also approximately orthogonal, i.e. $\mathbf{F}_{BB}^H\mathbf{F}_{BB} \approx \zeta^2\mathbf{I}_K$, where ζ^2 is a normalization factor. Similarly, we can find $\mathbf{W}_{BB}\mathbf{W}_{BB}^H \approx \xi^2\mathbf{I}_K$ and $\mathbf{W}_{BB}^H\mathbf{W}_{RF}^H\mathbf{W}_{RF}\mathbf{W}_{BB} \approx \mathbf{I}_K$. Let $\gamma^2 \triangleq \zeta^2\xi^2$, then (8) can be further simplified as

$$R \approx \log_2\left(\left|\frac{P\gamma^2}{K\sigma^2}\mathbf{W}_{RF}^H\mathbf{H}\mathbf{F}_{RF}\mathbf{F}_{RF}^H\mathbf{H}^H\mathbf{W}_{RF}\right|\right) \quad (9)$$

$$\overset{(a)}{=} K\log_2\left(\frac{P\gamma^2}{K\sigma^2}\right) + 2 \times \log_2\left(\left|\mathbf{W}_{RF}^H\mathbf{H}\mathbf{F}_{RF}\right|\right), \quad (10)$$

where (a) follows the fact that $|\mathbf{X}\mathbf{Y}| = |\mathbf{X}||\mathbf{Y}|$ when $\mathbf{X}$ and $\mathbf{Y}$ are both square matrices.

Therefore, the analog precoder and combiner design can be formulated as:

$$\{\mathbf{F}_{RF}^\star, \mathbf{W}_{RF}^\star\} = \arg \max_{\substack{\forall \mathbf{f}_{RF,l} \in \frac{1}{\sqrt{M_t}}\{\pm 1\}^{M_t} \\ \forall \mathbf{w}_{RF,l} \in \frac{1}{\sqrt{M_r}}\{\pm 1\}^{M_r}}} \log_2\left(\left|\mathbf{W}_{RF}^H\mathbf{H}\mathbf{F}_{RF}\right|\right). \quad (11)$$

Unfortunately, this binary analog beamformer design problem is a non-convex and NP-hard problem. Hence, we propose to further decompose this difficult optimization problem into a series of sub-problems, in which each sub-array pair is considered one by one, and the analog precoder and combiner for each pair are successively designed.

In particular, we define the singular value decomposition (SVD) of $\mathbf{H}$ as

$$\mathbf{H} = \mathbf{U}\boldsymbol{\Sigma}\mathbf{V}^H, \quad (12)$$

where $\mathbf{U}$ is an $N_r \times N_r$ unitary matrix, $\mathbf{V}$ is an $N_t \times N_t$ unitary matrix and $\boldsymbol{\Sigma}$ is a rectangular diagonal matrix of singular values arranged in a decreasing order on the diagonal. Due to the sparse nature of the mmWave channel, the matrix $\mathbf{H}$ is typically low rank. In particular, the effective rank of the channel serves as an upper bound for the number of data streams K that the channel can support. For convenience, we adopt a Matlab-like matrix indexing notation and let $\widehat{\mathbf{U}} \triangleq \mathbf{U}(:, 1:K)$ indicate the first K columns of matrix $\mathbf{U}$. Similarly, we define $\widehat{\boldsymbol{\Sigma}} \triangleq \boldsymbol{\Sigma}(1:K, 1:K)$ and $\widehat{\mathbf{V}} \triangleq \mathbf{V}(:, 1:K)$. Therefore, the channel $\mathbf{H}$ can be well approximated by retaining only the K strongest components $\mathbf{H} \approx \widehat{\mathbf{U}}\widehat{\boldsymbol{\Sigma}}\widehat{\mathbf{V}}^H$. Then, the objective in (11) can be converted to

$$\log_2\left(\left|\mathbf{W}_{RF}^H\mathbf{H}\mathbf{F}_{RF}\right|\right) \approx \log_2\left(\left|\mathbf{W}_{RF}^H\widehat{\mathbf{U}}\widehat{\boldsymbol{\Sigma}}\widehat{\mathbf{V}}^H\mathbf{F}_{RF}\right|\right). \quad (13)$$

Next, we denote $\mathbf{F}_{RF,\backslash l}$ as the precoding matrix excluding the l-th column $\mathbf{F}_{RF}(:, l)$ and $\mathbf{W}_{RF,\backslash l}$ as the combining matrix excluding the l-th column $\mathbf{W}_{RF}(:, l)$. The objective in (11) can be finally reformulated as:

$$\log_2\left(\left|\mathbf{W}_{RF}^H\mathbf{H}\mathbf{F}_{RF}\right|\right) \approx \log_2\left(\left|\mathbf{W}_{RF,\backslash l}^H\mathbf{H}\mathbf{F}_{RF,\backslash l}\right|\right) + \log_2\left(\left|\mathbf{W}_{RF}(:, l)^H\mathbf{G}_l\mathbf{F}_{RF}(:, l)\right|\right), \quad (14)$$

where $\mathbf{G}_l$ is the interference included channel matrix defined as

$$\mathbf{G}_l \triangleq \widehat{\mathbf{U}}(\alpha\mathbf{I}_K + \widehat{\boldsymbol{\Sigma}}\widehat{\mathbf{V}}^H\mathbf{F}_{RF,\backslash l}\mathbf{W}_{RF,\backslash l}^H\widehat{\mathbf{U}})^{-1}\widehat{\boldsymbol{\Sigma}}\widehat{\mathbf{V}}^H, \quad (15)$$

and α is a very small scalar to assure invertibility. Due to the limitation of space, the detailed derivation of (14) is ignored.

According to (14), if $\mathbf{F}_{RF,\backslash l}$ and $\mathbf{W}_{RF,\backslash l}$ are known, the objective is to maximize the second term on the right side. Note that $\mathbf{F}_{RF}(:, l)$ and $\mathbf{W}_{RF}(:, l)$ only have M_t and M_r non-zero elements due to the partially-connected structure, we reformulate the problem (11) as finding a corresponding precoder $\mathbf{f}_{RF,l}$ and combiner $\mathbf{w}_{RF,l}$ pair to conditionally maximize the achievable spectral efficiency:

$$\{\mathbf{f}_{RF,l}^\star, \mathbf{w}_{RF,l}^\star\} = \arg \max_{\substack{\mathbf{f}_{RF,l} \in \frac{1}{\sqrt{M_t}}\{\pm 1\}^{M_t} \\ \mathbf{w}_{RF,l} \in \frac{1}{\sqrt{M_r}}\{\pm 1\}^{M_r}}} \left|\mathbf{w}_{RF,l}^H\mathbf{Q}_l\mathbf{f}_{RF,l}\right|, \quad (16)$$

where $\mathbf{Q}_l$ is the corresponding $M_r \times M_t$ sub-matrix of $\mathbf{G}_l$ and is defined as

$$\mathbf{Q}_l \triangleq \mathbf{G}_l\left(\left(l-1\right)M_r + 1 : lM_r, \left(l-1\right)M_t + 1 : lM_t\right). \quad (17)$$

The optimization problem (16) can be solved through exhaustive search with exponential complexity $\mathcal{O}(2^{M_t M_r})$, which would not be affordable with large antenna arrays. Therefore, in the following we attempt to develop an efficient binary beamformer design with polynomial complexity in the number of antennas.

We first define the SVD of $\mathbf{Q}_l$ as

$$\mathbf{Q}_l = \sum_{i=1}^{K} \lambda_{l,i} \mathbf{p}_{l,i} \mathbf{g}_{l,i}^H, \tag{18}$$

where $\mathbf{p}_{l,i}$ and $\mathbf{g}_{l,i}$ are the i-th left and right singular vectors of $\mathbf{Q}_l$, respectively, and $\lambda_{l,i}$ is the i-th largest singular value, $\lambda_{l,1} \geq \lambda_{l,2} \geq \ldots \geq \lambda_{l,K}$. Then, the objective in (16) can be rewritten as

$$|\mathbf{w}_{RF,l}^H \mathbf{Q}_l \mathbf{f}_{RF,l}| = \left| \sum_{i=1}^{K} \lambda_{l,i} \mathbf{w}_{RF,l}^H \mathbf{p}_{l,i} \mathbf{g}_{l,i}^H \mathbf{f}_{RF,l} \right|. \tag{19}$$

If we utilize a rank-1 approximation by keeping only the strongest term, i.e. $\mathbf{Q}_l \approx \lambda_{l,1} \mathbf{p}_{l,1} \mathbf{g}_{l,1}^H$, the optimization function in (16) can be approximated by

$$\left\{ \mathbf{f}_{RF,l}^\star, \mathbf{w}_{RF,l}^\star \right\} = \arg \max_{\substack{\mathbf{f}_{RF,l} \in \frac{1}{\sqrt{M_t}} \{\pm 1\}^{M_t} \\ \mathbf{w}_{RF,l} \in \frac{1}{\sqrt{M_r}} \{\pm 1\}^{M_r}}} \left| \mathbf{w}_{RF,l}^H \mathbf{p}_{l,1} \mathbf{g}_{l,1}^H \mathbf{f}_{RF,l} \right|. \tag{20}$$

It is noted that the performance loss caused by the rank-1 approximation is small and can be ignored due to the interference-included equivalent channel $\mathbf{Q}_l$ is low-rank under the mmWave circumstance. Now, the joint optimization problem (20) can be decoupled into individually designing the analog precoder $\mathbf{f}_{RF,l}$ and combiner $\mathbf{w}_{RF,l}$:

$$\mathbf{f}_{RF,l}^\star = \arg \max_{\mathbf{f}_{RF,l} \in \frac{1}{\sqrt{M_t}} \{\pm 1\}^{M_t}} \left| \mathbf{f}_{RF,l}^H \mathbf{g}_{l,1} \right|, \tag{21}$$

$$\mathbf{w}_{RF,l}^\star = \arg \max_{\mathbf{w}_{RF,l} \in \frac{1}{\sqrt{M_r}} \{\pm 1\}^{M_r}} \left| \mathbf{w}_{RF,l}^H \mathbf{p}_{l,1} \right|. \tag{22}$$

However, solving (21) and (22) by exhaustive search still has exponential complexity in the number of antennas. In order to further reduce the complexity without a significant loss of performance, we propose to construct a smaller dimension candidate beamformer set, from which the optimal beamformer can be found with quadratic complexity. In the following, we present this algorithm for the precoder design (21) as an example, while the combiner design (22) follows the same procedure.

We introduce an auxiliary variable $\phi \in [-\pi, \pi)$ and reformulate the optimization problem (21) as:

$$\left\{ \phi^\star, \mathbf{f}_{RF,l}^\star \right\} = \arg \max_{\substack{\phi \in [-\pi, \pi) \\ \mathbf{f}_{RF,l} \in \frac{1}{\sqrt{M_t}} \{\pm 1\}^{M_t}}} \mathfrak{Re} \left\{ \mathbf{f}_{RF,l}^H \mathbf{g}_{l,1} e^{-j\phi} \right\} \tag{23}$$

$$= \arg \max_{\substack{\phi \in [-\pi, \pi) \\ \mathbf{f}_{RF,l} \in \frac{1}{\sqrt{M_t}} \{\pm 1\}^{M_t}}} \sum_{i=1}^{M_t} \mathbf{f}_{RF,l}(i) |\mathbf{g}_{l,1}(i)| \cos(\phi - \psi_i), \tag{24}$$

where ψ_i denotes the phase of $\mathbf{g}_{l,1}(i)$. Obviously, given any $\phi \in [-\pi, \pi)$, the corresponding binary precoder that maximizes (24) is

$$\mathbf{f}_{RF,l}(i) = \frac{1}{\sqrt{M_t}} \text{sign} \left(\cos \left(\phi - \psi_i \right) \right), i = 1, \ldots, M_t. \tag{25}$$

With the conditionally optimal $\mathbf{f}_{RF,l}$ for any given ϕ shown in (25), we will now show that we can always construct a set of M_t candidate binary precoders $\mathcal{F}_l \triangleq \{\mathbf{f}_{l,1}, \ldots, \mathbf{f}_{l,M_t}\}$ and guarantee $\mathbf{f}_{RF,l}^\star \in \mathcal{F}_l$. Then, the maximization in (21) can be carried out over a set of only M_t candidates without loss of performance.

We first define the angles $\widehat{\psi}_i$, $i = 1, \ldots, M_t$, as

$$\widehat{\psi}_i \triangleq \begin{cases} \psi_i - \pi, & \text{if } \psi_i \in \left[\frac{\pi}{2}, \frac{3\pi}{2} \right), \\ \psi_i, & \text{if } \psi_i \in \left[-\frac{\pi}{2}, \frac{\pi}{2} \right), \end{cases} \tag{26}$$

so that $\widehat{\psi}_i \in [-\frac{\pi}{2}, \frac{\pi}{2})$. Then, we map the angles $\widehat{\psi}_i$ to $\widetilde{\psi}_i$, $i = 1, \ldots, M_t$, which are rearranged in ascending order, i.e. $\widetilde{\psi}_1 \leq \widetilde{\psi}_2 \leq \ldots \leq \widetilde{\psi}_{M_t}$. Because of the periodicity of the cosine function, the maximization problem (24) with respect to ϕ can be carried out over any interval of length π. If we construct M_t non-overlapping sub-intervals $[\widetilde{\psi}_1 - \frac{\pi}{2}, \widetilde{\psi}_2 - \frac{\pi}{2}), [\widetilde{\psi}_2 - \frac{\pi}{2}, \widetilde{\psi}_3 - \frac{\pi}{2}), \ldots, [\widetilde{\psi}_{M_t} - \frac{\pi}{2}, \widetilde{\psi}_1 + \frac{\pi}{2})$, then the optimal $\phi^\star$ must be located in one of M_t sub-intervals since the full interval is $[\widetilde{\psi}_1 - \frac{\pi}{2}, \widetilde{\psi}_1 + \frac{\pi}{2})$ of length π. Therefore, the optimization problem (24) can be solved by examining each sub-interval separately.

Assuming the optimal $\phi^\star$ is in the k-th sub-interval, the corresponding optimal binary precoder can be obtained by (25) as $\widetilde{\mathbf{f}}_{l,k}(i) = \frac{1}{\sqrt{M_t}} \text{sign} \left(\cos \left(\phi^\star - \widetilde{\psi}_i \right) \right)$, $i = 1, \ldots, M_t$, and has the form

$$\widetilde{\mathbf{f}}_{l,k} = \frac{1}{\sqrt{M_t}} [\underbrace{1 \ldots 1}_{k} \underbrace{-1 \ldots -1}_{M_t - k}]^T. \tag{27}$$

After that, given the inverse sorting that maps $\widetilde{\psi}_i$ to $\widehat{\psi}_i$, we rearrange the corresponding elements of $\widetilde{\mathbf{f}}_{l,k}$ and obtain $\widehat{\mathbf{f}}_{l,k}$. Then, based on the relationship between ψ_i and $\widehat{\psi}_i$ defined in (26), we can achieve the conditionally optimal precoder $\mathbf{f}_{l,k}$ by

$$\mathbf{f}_{l,k}(i) \triangleq \begin{cases} -\widehat{\mathbf{f}}_{l,k}(i), & \text{if } \psi_i \in \left[\frac{\pi}{2}, \frac{3\pi}{2} \right), i = 1, \ldots, M_t, \\ \widehat{\mathbf{f}}_{l,k}(i), & \text{if } \psi_i \in \left[-\frac{\pi}{2}, \frac{\pi}{2} \right), i = 1, \ldots, M_t, \end{cases} \tag{28}$$

for the case that $\phi^\star$ is in the k-th sub-interval.

Since the optimal $\phi^\star$ must be located in one of M_t sub-intervals, we can obtain M_t conditionally optimal precoders by examining all M_t sub-intervals and construct a candidate precoder set $\mathcal{F}_l$ as

$$\mathcal{F}_l \triangleq \{\mathbf{f}_{l,1}, \ldots, \mathbf{f}_{l,M_t}\}, \tag{29}$$

which must contain the optimal precoder $\mathbf{f}_{RF,l}^\star$. Therefore, without loss of performance, the problem in (21) can be transformed to an equivalent maximization task over only the set $\mathcal{F}_l$

$$\mathbf{f}_{RF,l}^{\star} = \arg\max_{\mathbf{f}_{RF,l}\in\mathcal{F}_l} \left|\mathbf{f}_{RF,l}^{H}\mathbf{g}_{l,1}\right|. \quad (30)$$

Similarly, we can also construct a candidate analog combiner set $\mathcal{W}_l$ and obtain $\mathbf{w}_{RF,l}^{\star}$ by the same procedure.

The rank-1 solution returned by (30) is based on the rank-1 approximation of the interference-included equivalent channel $\mathbf{Q}_l$. The approximation of $\mathbf{Q}_l$ may cause a performance degradation when we revisit the original problem (16). Therefore, in order to enhance the performance, we propose to jointly select the precoder and combiner over candidate sets $\mathcal{F}_l$ and $\mathcal{W}_l$ as

$$\left\{\mathbf{f}_{RF,l}^{\star}, \mathbf{w}_{RF,l}^{\star}\right\} = \arg\max_{\substack{\mathbf{f}_{RF,l}\in\mathcal{F}_l \\ \mathbf{w}_{RF,l}\in\mathcal{W}_l}} \left|\mathbf{w}_{RF,l}^{H}\mathbf{Q}_l\mathbf{f}_{RF,l}\right|, \quad (31)$$

which may return the rank-1 or a better solution with polynomial complexity.

B. Digital Precoder and Combiner Design

After all analog precoder-combiner pairs have been determined, we can obtain the effective baseband channel $\widetilde{\mathbf{H}}$ as

$$\widetilde{\mathbf{H}} \triangleq \left(\mathbf{W}_{RF}^{\star}\right)^{H}\mathbf{H}\mathbf{F}_{RF}^{\star}. \quad (32)$$

For the baseband precoder and combiner design, we define the SVD of the effective baseband channel $\widetilde{\mathbf{H}}$ as

$$\widetilde{\mathbf{H}} = \widetilde{\mathbf{U}}\widetilde{\mathbf{\Sigma}}\widetilde{\mathbf{V}}^{H}, \quad (33)$$

where $\widetilde{\mathbf{U}}$ and $\widetilde{\mathbf{V}}$ are $K\times K$ unitary matrices, $\widetilde{\mathbf{\Sigma}}$ is an $K\times K$ diagonal matrix of singular values. Then, in order to further enhance the spectral efficiency, an SVD-based baseband digital precoder and combiner are employed:

$$\mathbf{F}_{BB}^{\star} = \widetilde{\mathbf{V}}, \quad (34)$$

$$\mathbf{W}_{BB}^{\star} = \widetilde{\mathbf{U}}. \quad (35)$$

IV. Simulation Results

In this section, we illustrate the simulation results of the proposed joint hybrid precoder and combiner design. Both transmitter and receiver are equipped with 64-antenna ULAs, where antenna spacing is $d = \frac{\lambda}{2}$. The numbers of RF chains at transmitter and receiver are $K = 4$. The channel parameters are set as $N_{cl} = 10$ clusters, $N_{ray} = 5$ rays per cluster, and the average power of the i-th cluster is $\sigma_{\alpha,i}^{2} = c\frac{7}{10}^{i}$ where $c = (\sum_{i=1}^{N_{cl}}(\frac{7}{10})^{i})^{-1}N_{cl}$. The azimuths of the AoAs/AoDs within a cluster are assumed to be Laplacian-distributed with angle spreads of $\sigma_{\theta_i^r} = \sigma_{\theta_i^t} = 0.5°$. The mean cluster AoDs are assumed to be uniformly distributed over $[0, 2\pi]$, while the mean cluster AoAs are uniformly distributed over an arbitrary $\frac{\pi}{3}$ sector.

Fig. 2 shows the spectral efficiency versus SNR over 10^6 channel realizations. For the comparison purpose, we include two state-of-the-art algorithms: *i*) Spatially sparse precoding (SSP) for fully-connected architectures [7] and *ii*) successive interference cancelation (SIC) based approach for partially-connected architectures [4]. Note that the SSP algorithm is based on a codebook of 128 resolution and the SIC approach uses infinite-resolution PSs. For fair comparison, we also plot the spectral efficiency of the one-bit quantized version of SIC (SIC-Q), where the binary beamformers are obtained by directly quantizing each element of analog beamformers designed by SIC to the finite set. The optimal full-digital beamforming scheme based on SVD is also plotted as the performance benchmark. It can be observed from Fig. 2 that our proposed algorithm can achieve satisfactory performance close to the SIC with infinite-resolution PSs and outperform SIC-Q using one-bit PSs. Fig. 3 illustrates the impact of the number of transmit antennas on the spectral efficiency performance and similar conclusions can be drawn.

Now we turn to evaluate the energy efficiencies of different beamforming schemes. For the full-digital scheme, the energy efficiency is defined as

$$\eta_D = \frac{R}{P + P_{BB} + N_t P_{RF}}, \quad (36)$$

where P_{BB} and P_{RF} are the powers consumed by the baseband processor and a RF chain, respectively. For the fully-connected architecture with the SSP algorithm, the energy efficiency is given by

$$\eta_{SSP} = \frac{R}{P + P_{BB} + KP_{RF} + KN_t P_{PS}^{h}}, \quad (37)$$

where P_{PS}^{h} is the power consumed by a high-resolution PS. The energy efficiency for partially-connected architecture with SIC algorithm is

$$\eta_{SIC} = \frac{R}{P + P_{BB} + KP_{RF} + N_t P_{PS}^{h}}. \quad (38)$$

Finally, for our proposed algorithm as well as the SIC-Q approach, the energy efficiency can be computed by

$$\eta_P = \frac{R}{P + P_{BB} + KP_{RF} + N_t P_{PS}^{o}}, \quad (39)$$

where P_{PS}^{o} is power consumption of a one-bit PS. In the simulation, we set the transmit power P = 500mW, and P_{BB} = 200mW, P_{RF} = 300mW [12]. The power consumption of different resolution PS is P_{PS}^{h} = 45mW [13] and P_{PS}^{o} = 10mW [12]. Fig. 4 illustrates the energy efficiency versus the number of RF chains K. It can be observed that the partially-connected structures have significant advantages of energy efficiency. Moreover, the proposed algorithm can always achieve much higher energy efficiency than its competitors. Then, we also present energy efficiency versus the number of transmit antennas N_t in Fig. 5, from which we can find that the proposed algorithm can maintain the best energy efficiency performance with the growing number of antennas.

V. Conclusions

This paper considered the problem of hardware-efficiency hybrid precoder and combiner design in the partially-

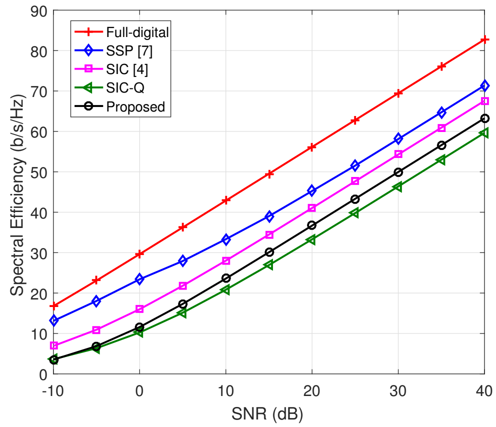

Fig. 2. Spectral efficiency versus SNR ($N_t = 64$, $N_r = 64$, $K = 4$).

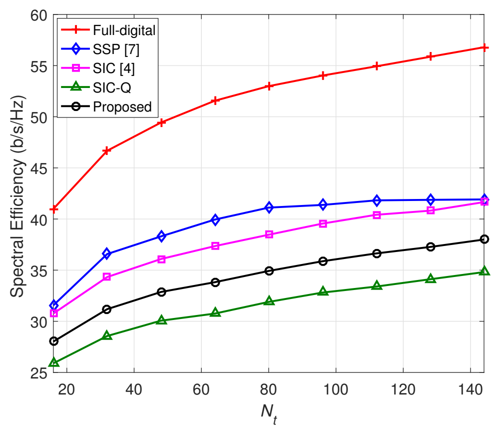

Fig. 3. Spectral efficiency versus N_t ($N_r = 32$, $K = 4$, SNR=20dB).

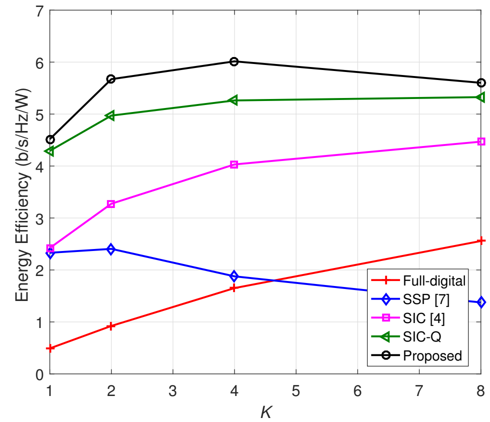

Fig. 4. Energy efficiency versus K ($N_t = 64$, $N_r = 64$).

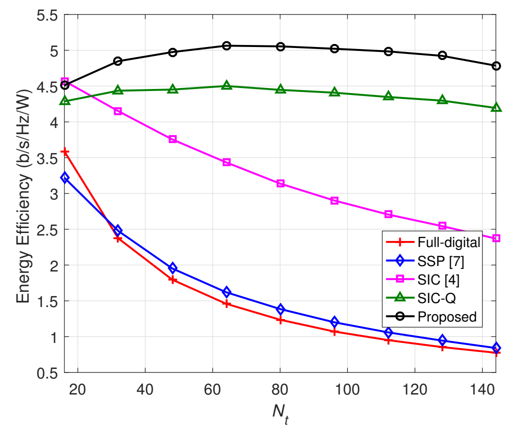

Fig. 5. Energy efficiency versus N_t ($N_r = 32$, $K = 4$).

connected hybrid beamforming architecture with one-bit quantized PSs. We introduced a novel binary analog precoder and combiner optimization algorithm with polynomial complexity in the number of antennas. Then, the digital precoder and combiner were computed based on the obtained effective baseband channel to further maximize the spectral efficiency. Simulation results illustrated that the proposed joint hybrid precoder and combiner design can achieve satisfactory spectral efficiency performance and have significant energy efficiency improvement.

References

[1] Z. Pi and F. Khan, "An introduction to millimeter-wave mobile broadband systems," *IEEE Commun. Mag.*, vol. 49, no. 6, pp. 101-107, June 2011.

[2] T. Rappaport, S. Sun, R. Mayzus, H. Zhao, Y. Azar, K. Wang, G. N. Wong, J. K. Schulz, M. Samimi and F. Gutierrez "Millimeter wave mobile communications for 5G cellular: It will work!" *IEEE Access*, vol. 1, pp. 335-349, 2013.

[3] R. W. Heath Jr., N. González-Prelcic, S. Rangan, W. Roh, and A. M. Sayeed, "An overview of signal processing techniques for millimeter wave MIMO systems," *IEEE J. Sel. Topics Signal Process.*, vol. 10, no. 3, pp. 436-453, April 2016.

[4] X. Gao, L. Dai, S. Han, C.-L. I, and R. W. Heath Jr., "Energy-efficient hybrid analog and digital precoding for mmWave MIMO systems with large antenna arrays," *IEEE J. Sel. Areas Commun.*, vol. 34, no. 4, pp. 998-1009, April 2016.

[5] X. Yu, J.-C. Shen, J. Zhang, and K. B. Letaief, "Alternating minimization algorithms for hybrid precoding in millimeter wave MIMO systems," *IEEE J. Sel. Topics Signal Process.*, vol. 10, no. 3, pp. 485-500, April 2016.

[6] F. Sohrabi and W. Yu, "Hybrid digital and analog beamforming design for large-scale antenna arrays," *IEEE J. Sel. Topics Signal Process.*, vol. 10, no. 3, pp. 501-513, April 2016.

[7] O. E. Ayach, S. Rajagopal, S. Abu-Surra, Z. Pi, and R. W. Heath Jr., "Spatially sparse precoding in millimeter wave MIMO systems," *IEEE Trans. Wireless Commun.*, vol. 13, no. 3, pp. 1499-1513, Mar. 2014.

[8] A. Alkhateeb and R. W. Heath Jr., "Frequency selective hybrid precoding for limited feedback millimeter wave systems," *IEEE Trans. Commun.*, vol. 64, no. 5, pp. 1801-1818, May 2016.

[9] X. Gao, L. Dai, C. Yuen, and Z. Wang, "Turbo-like beamforming based on Tabu search algorithm for millimeter-wave massive MIMO systems," *IEEE Trans. Veh. Technol.*, vol. 65, no. 7, pp. 5731-5737, July 2016.

[10] O. El Ayach, R. W. Heath Jr., S. Rajagopal, and Z. Pi, "Multimode precoding in millimeter wave MIMO transmitters with multiple antenna sub-arrays," in *Proc. IEEE Global Commun. Conf. (GLOBECOM)*, Atlanta, GA, Dec. 2013, pp. 3476-3480.

[11] G. N. Karystinos and D. A. Pados, " Rank-2-optimal adaptive design of binary spreading codes," *IEEE Trans. Inf. Theory*, vol. 53, no. 9, pp. 3075-3080, Sept. 2007.

[12] X. Gao, L. Dai, Y. Sun, S. Han, and C.-L. I, "Machine learning inspired energy-efficient hybrid precoding for mmWave massive MIMO systems," in *Proc. IEEE Int. Conf. Commun. (ICC)*, Paris, France, May 2017.

[13] R. Méndez-Rial, C. Rusu, N. González-Prelcic, and A. Alkhateeb, "Hybrid MIMO architectures for millimeter wave communications: Phase shifters fo switches?" *IEEE Access*, vol. 4, pp. 247-267, Jan. 2016.